Article
https://doi.org/10.31489/2024PH4/123-132
UDC 535.015
Received: 00.00.2024
Accepted: 00.00.2024

A.A. Zvekov[1*], A.V. Kalenskii[1], A.V. Ivanov[1], A.P. Borovikova[1], D.R. Nurmuhametov[2]

[1]*Kemerovo State University, Kemerovo, Russia*
[2]*Federal Research Center of Coal and Coal Chemistry SB RAS, Kemerovo, Russia*
([*]Corresponding author's e-mail: aazvekov@yandex.ru)

Non-linear optic properties of colloids prepared by metal targets' laser ablation in dimethylsulfoxide

A set of colloids on the base of aluminum, nickel, and zinc was prepared by their targets' ablation in dimethylsulfoxide medium. The samples were characterized with UV-vis spectroscopy, transmission electron microscopy, and dynamic light scattering methods. The substantial non-linear attenuation was observed with z-scan techniques using pulsed neodymium laser (532 nm, 14 ns). The transmittance of the samples diminishes when the light intensity increases. The photoacoustic signal amplitude rises with the energy density increasing according to the sublinear law. The dependencies of the attenuation linear coefficient and pressure generation efficiency on the pulse energy density were described with power laws with a threshold of the effect and the parameters were estimated. We found out that the dependencies' parameters change when the colloids were diluted. The pear pressure was determined using ferrocene as a calibration standard. It is shown that the values of peak pressure could not be explained in terms of thermal expansion of the substance. The results are discussed in terms of the non-linear attenuation mechanism concerned on the substance evaporation leading to vapor bubbles formation around the nanoparticles.

Keywords: ablation, dimethylsulfoxide, non-linear light attenuation, photoacoustic spectroscopy, laser irradiation.

Introduction

Non-linear light attenuation poses an important place among the non-linear optics phenomena because it can be used in the intensity selection devices. Colloid metals and systems based on them performs significant dependence of the transmittance on the energy density of the pulsed [1] or power density of the continuous wave laser irradiation [2]. Numerous results were obtained in that way that make it possible to solve applied problems.

Silver nanoparticles were obtained by metal target in ethanol ablation and their influence on the curcumin dye fluorescence and nonlinear light absorption was studied [3]. The authors found out that fluorescence intensity increases linearly and normalized transmittance in focus decreases almost linearly with silver nanoparticles concentration increasing while the fluorescence decay time remains unchanged. The silver nanoparticles coated with silica are able to shift the nonlinear attenuation of methylene blue depending on the dye to nanoparticles concentrations ratio [4]. At low ratio the bleaching is observed changed to absorption increasing at the high ones. The effect is discussed as increasing in the triplet state absorption cross section of the dye. Gold and platinum nanoparticles were prepared with laser ablation synthesis as well as the respective bimetallic nanoparticles with laser molding of nanoparticles [5]. These nanoparticles show significant non-linear absorption and refraction and they are heated efficiently with stationary laser at the wavelength 403 nm. The silver coated gold nanoparticles were synthesized in [6] by metals reduction with Jatoba extract. The light absorption of prepared colloid was tested with thermal lens techniques. The boron- Antimony -europium glasses containing silver nanoparticles whose non-linear absorption and refraction coefficients are linearly dependent on silver content were prepared in [7]. It was shown in [8] that commercial silver and zinc nanopartciles performs significant non-linear light attenuation at the wavelength 1550 nm.

At the same time, the definite mechanisms of non-linear attenuation of light remain unclear in many cases that lead to insufficiently predictable results when the sample parameters are changed. The concentration of metal nanoparticles influence is seldom discussed as well as the effects accompanying the non-linear attenuation of laser beams. Thermalization always accompanies the absorption of laser irradiation [9], so their study as photoacoustic effect [10] or themal lensing [6] can give essential information on the absorption features.

The aim of the work is to study the non-linear light attenuation and accompanying effects in the model metal colloids prepared with laser ablation method.

The main tasks are:

1. Preparation of the colloids on the aluminum, nickel, and zinc base with ablation method.
2. Research into optic characteristics and photoacoustic response of these colloids varying the laser light intensity and solution concentration.
3. Results description with empiric models and discussion.

We used ablation products of aluminum, zinc, and nickel in dimethylsulfoxide (DMSO) as experimental samples. The methods of noble metal nanoparticles synthesis with ablation under the layer of water or organic solvents are descried in [10–12]. Aluminum nanoparticles formed by metal ablation in chloroform and carbon tetrachloride showing pronounced non-linear attenuation were prepared in [13]. One of the problems in the ablation under solvent layer approach is byproducts formation. Utilization of solvents less reactive than water is one of the ways to inhibit formation of the oxides. Increasing in viscosity of the solvent hiders the sedimentation. From that point of view, utilization of DMSO which is more viscose than water is able to be beneficial in the products properties. At the same time DMSO decomposition could give additional byproducts such as carbon [14], sulfides or oxides. Silver sulfide forms in the case of silver ablation in DMSO, for instance [15].

Experimental section

Synthesis of the nanoparticles, z-scan and photoacoustic measurements were done with YAG-Nd laser Solar LQ929 operated in the Q-switch mode with pulse duration full width at half maximum 14 ns. A round 8 mm aperture was used for cutting the peripheral part of the beam central part of the beam, so the intensity fallen on the sample was almost uniform in the spot.

Colloids were synthesized by pulsed irradiation with main wavelength of YAG-Nd laser of metal targets sink in DMSO in a beaker. The pulses frequency was 10 Hz. The solvent was agitated with magnetic stirrer during the irradiation. Horizontal laser beam was focused on the vertical target with a lens having focus length 5 cm so the spark at the target surface was pronounced. The energy of the beam was taken as 50 mJ initially with subsequent increasing as the turbidity of the solution hindered the ablation. The beaker was placed on the table with variable height which allowed us to shift the point of the beam action on the target surface. The turbid yellow-to-gray colloid solution formed as a result of laser pulsed irradiation of the target. Aluminum concentration estimated by the target mass losses was 196 μg/ml. Tough partial sedimentation of the solid was observed after the storage the colloid could be homogenized with ultrasonification. The colloidal products of zinc and nickel targets were prepared the same way. The concentration of metals in DMSO were estimated at 102 μg/ml and 100 μg/ml in the cases of zinc and nickel respectively. The photoacoustic and dynamic light scattering measurements were conducted with colloids diluted 12.5 times that did not suffer from sedimentation.

The samples were characterized with transmission electron microscopy (TEM) using electron microscope JEOL-2100. Dynamic light scattering was done with Malvern Zetasizer Nano ZS (Malvern Instruments). The UV-vis spectra of the colloids were measured with the spectrophotometer Shimadzu UV-3600.

The photoacoustic effect and laser beam attenuation by colloid ablation products was studied on the facility based on YAG-Nd laser operating in the Q-switch mode (pulse duration 14 ns, wavelength 532 nm). The cuvette filled with colloid solution was placed on the stage that could be moved along the optical rail. In the case of photoacoustic measurements the cuvette thickness was 2 cm and the sample was situated at the lens focus (f=25 см). The beam diameter in the focal plane was estimated at 485 μm. The pulse energy varied with the neutral light filters placed on the beam path. The photoacoustic signal was measured with a sensor on the PZT ceramics whose aluminum “acoustic delay” sinks in the colloid from the top at the center or near the front glass of the cuvette. The voltage generated by the acoustic sensor when it received the acoustic wave was transferred to the resistance of the oscilloscope. We used ferrocene solution in DMSO (5 mg/ml) as a standard.

The photoacoustic signals were processed as follows. The noises were eliminated with the moving average approach. This method has an essential drawback that is diminishing of the maximum and minimum values in the absolute scale. For that reason, we approximated the signal near these points with parabolic functions determining the extreme values. The dispersion and confidence interval at the confidence probability level 95 % were calculated for each extreme value.

The non-linear attenuation was studied with open aperture z-scan method using the same facility by moving the sample stage along the optic rail. We did not dilute the colloidal solutions in the case using the cuvette with sample thickness 1 cm. The energy of the laser pulse was determined with OPHIR Photonics

detector. The beam radius at the sample surface was determined by the spot diameter left on the photofilm situated in front of the cuvette. The radii were approximated with Raleigh equation; the radius in the focus was estimated as 263 μm and the confocal distance as 1.43 cm. The measurements of the transmittance and photoacoustic signal were done 5 times for each conditions used.

Results

TEM images of the aluminum and nickel ablation products in DMSO show metal nanoparticles free or covered by substance with lower density (Fig. 1).

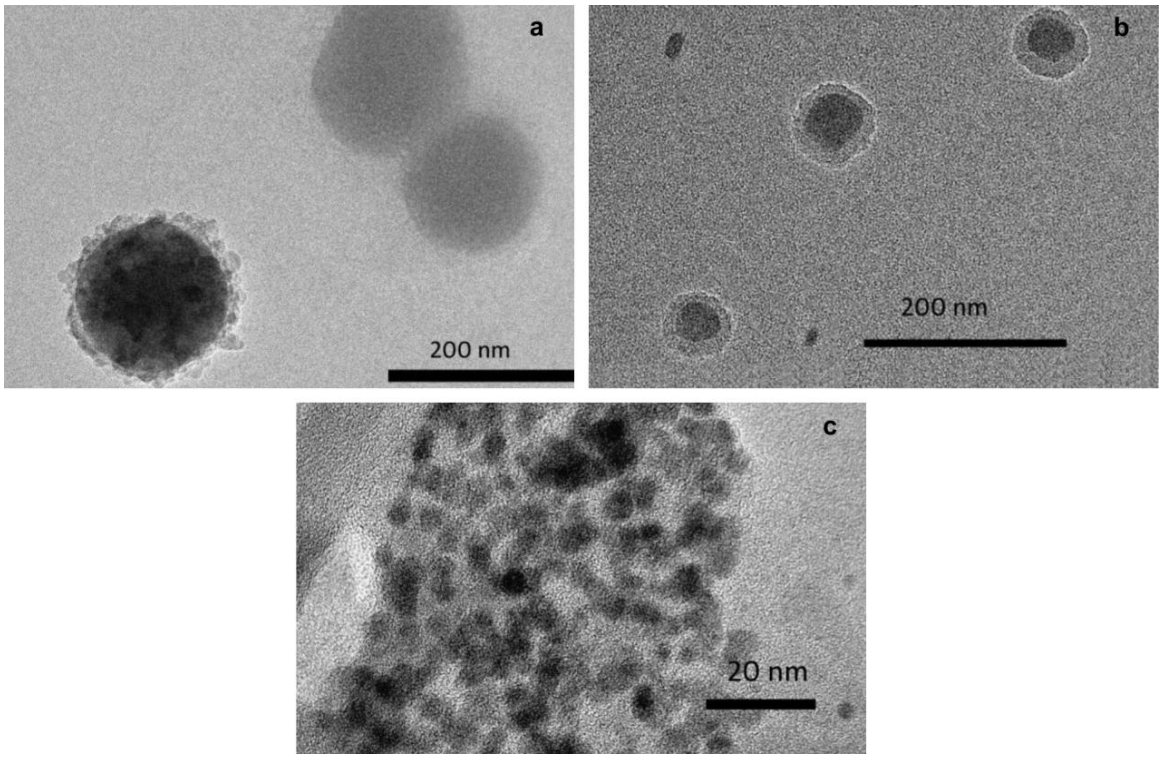

Figure 1. TEM images of aluminum (a), nickel (b), and zinc (c) colloid ablation products in DMSO.

In the aluminum case small particles with interplane distance about 0.6 nm were found, which is close to interplane distance for one of the carbon forms [16]. TEM images of sinc ablation products show agglomerates of extremely fine nanoparticles.

The optical attenuation spectra of the systems studied are presented in Figure 2 (cuvette thickness was 1 cm).

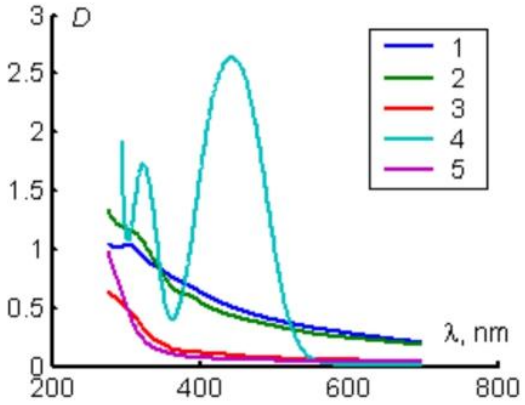

Figure 2. Attenuation spectra of zinc (1), nickel (2) and aluminum (3 diluted 10 times), and ferrocene in DMSO

The significant background level in the high wavelength area is observed that can be linked with carbon particles formation of metal particles covered with carbon shell [14]. The sulfide formation, spectrum of which is affected significantly by the stochiometry [17], while absorption maximum is situated near 300 nm [18], is possible in the zinc case. Nickel can also produce sulfides and oxides as ablation byproducts.

The dynamic light scattering results are presented in Table 1.

Table 1

Particle sized determined with dynamic light scattering

№	Target	Particles size, nm			
		By *I*	Rel. peak area, %	By *N*	Rel. peak area, %
1	Zn	1.1±0.4 340±210	18.0 82.0	0.8±0.2	100
	Zn (US)	500±100	100	480±110	100
2	Ni	170±36 500±100	4.6 95.4	164±39 460±100	16.1 83.9
	Ni (US)	265±80 530±500	97.4 2.6	240±80	100.0
3	Al	58±11 200±50	12.3 87.7	47±10 190±50	96.9 3.1

The aluminum ablation products are nanoparticles with typical diameter 47 nm and their agglomerates of the size about 190 nm. The dymanic aggregation or sedimentation were not found in the aluminum ablation products' case. Zinc ablation products have typical size 1 nm, though these small particles are strongly agglomerated. The agglomerate size in the nickel case is 460 nm. Both zinc and nickel ablation products agglomeration extent is changed by ultrasonification that evidences the unstability of these colloids.

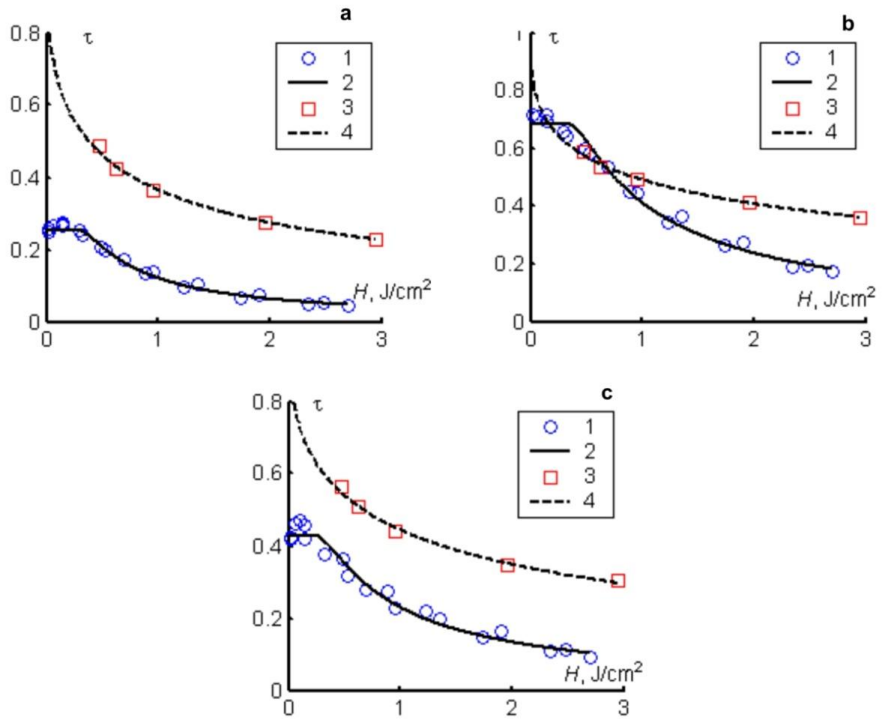

Figure 3. The trasmittance dependence of aluminum (a), nickel (b), and zinc (c) colloid ablation products on the pulse energy density measured for initial samples in 1 cm cuvette (1) and diluted in 12.5 times in 2 cm cuvette (3) with their approximation (2, 4).

Figure 3 presents the transmittance of the colloids of the laser beam at the wavelength 532 nm versus its energy density. The energy density was corrected by the beam reflectance at the cuvette wall taking into account. The data were measured with z-scan method and as additional information found in the photoacoustic

experiments. The increasing in the laser pulse energy density makes the transmittance decrease for both three systems studied. We assumed the power law dependence of the attenuation linear coefficient on the energy density with some effect threshold H_c one arrives at the following equation for transmittance:

$$\mu = \mu_0 \cdot \begin{cases} 1, H < H_c, \\ (H/H_c)^n, H \geq H_c \end{cases}, \quad (1)$$

where μ_0 is the attenuation linear coefficient in the Beer's law range (linear range), n is the power value, and H is incident energy density. Using the following transmittance dependence on the energy density was derived:

$$\tau = \begin{cases} \exp(-\mu_0 l), H_0 \leq H_c, \\ \frac{H_c}{H_0} \exp\left[-\mu_0 l + \frac{1}{n} \cdot \left(1 - \left(\frac{H_c}{H_0}\right)^n\right)\right], H_c < H_0 \leq H_c \cdot (1 - n\mu_0 l)^{1/n}, \\ \left[1 + n\mu_0 l \cdot \left(\frac{H_0}{H_c}\right)^n\right]^{-1/n}, H_0 > H_c \cdot (1 - n\mu_0 l)^{1/n} \end{cases} \quad (2)$$

where $H_0 = H_{inc} \cdot (1 — \rho_{cell})$ is energy density on the front boundary of the sample which is the incident one corrected by the cell wall reflection ($\rho_{cell} \approx 10$ %).

The approximation results are shown in Figure 3 at the sample thickness 1 cm (initial concentration) with solid lines. The respective variable parameters are presented in Table 2. In the aluminum ablation product case the attenuation coefficient in the Beer's law range found with spectrophotometrical approach and extrapolated in the z-scan measurements coincide. The spectrophotometry gives 1.9 higher the linear attenuation coefficient in the Beer's limit than z-scan results' extrapolations in the nickel case, while for zinc ablation products the difference is about 5 %. This discrepancy evidences the instability of the colloids and changing of their properties during the storage, agreeing with the conclusion of the ultrasonification influence on the average aggregates size estimated with dynamic light scattering.

The transmission coefficients of the colloid ablation products 12.5 times diluted in the cuvette with 2 cm thickness are shown in Figure 3. These results were obtained along with the photoacoustic data, so the linear range was not reached, as the photoacoustic signal was too low in it. For that reason, the linear attenuation coefficient in the Beer's range was taken as the determined in the z-scan measurement divided by the dilution coefficient. The approximated dependencies are presented as dashed curves in Figure 3; the respective parameters determined could be found in Table 2. The comparison of the parameters determined in z-scan and photoacoustic experiments revealed that the critical energy density of the non-linear attenuation decreases by order of magnitude and power n decreases in 2-3 times for diluted solutions. The power n is a strong parameter, while critical energy density depends on the linear absorption coefficient in the Beer's range. The colloid ablation products of nickel and zinc targets are rather instable, so the critical energy densities for such colloids could vary in 0.5–2 times. Nonetheless, the conclusion on the critical energy density diminishing after the dilution is valid for every system studied.

The typical photoacoustic signal read with an oscilloscope is shown in Figure 4. The nickel target ablation product was used when this curve was measured; the sensor was situated in front of the cuvette; the energy density was 0.47 J/cm^2.

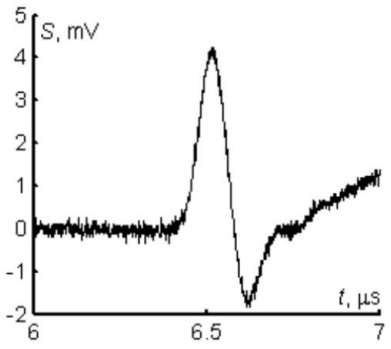

Figure 4. The typical photoacoustic signal

The first maximum on the photoacoustic curve is concerned on the compression wave due to the substance expansion in the irradiated zone. The maximum amplitude is linked with the linear absorption coefficient and energy density of the pulse. The ferrocene does not luminescence at all, so the thermal yield in its case is 1, and pressure amplitude could be estimated as (3):

$$p = \frac{\mu_a \rho c_s^2 \beta H_0}{a c_p} \int_{x_0}^{x_0+a} \exp(-\mu_a x) dx = \frac{\rho c_s^2 \beta H \cdot \exp(-\mu_a x_0)}{a c_p} \cdot [1 - \exp(-\mu_a a)], \quad (3)$$

where μ_a = 0.48 cm^{-1} is linear absorption coefficient of the ferrocene solution, l is cuvette thickness (2 cm), a is effective layer thickness forming the pressure wave influencing the sensor, w is radius of the laser beam at the cuvette center, c_p = 2.15 J/(cm^{3}K) is volumic heat capacity of DMSO, ρ =1.0955 g/cm^3 is density of DMSO, β = 8.8·10^{-4} K^{-1} is thermal expansion coefficient of DMSO [19]. The starting integration point was taken as 0, or (l — a)/2, or (l — a) depending on the sensor position at the front, center or rear point of the cuvette.

The photoacoustic signals measured at the lowest energy density value for ferrocene solution locating the sensor at the front, center, rear points of the cuvette gave us valuer of a parameter. The respective amplitudes were 1.36, 1.63, and 1.04 mV that gives the area value a= 1.1 cm at the experimental ferrocene solution linear absorption coefficient 0.48 cm^{-1}.

The amplitude of the photoacoustic signal dependences on the energy density of the laser pulse at the sensor position in the front and center points of the cuvette are shown in Figure 5.

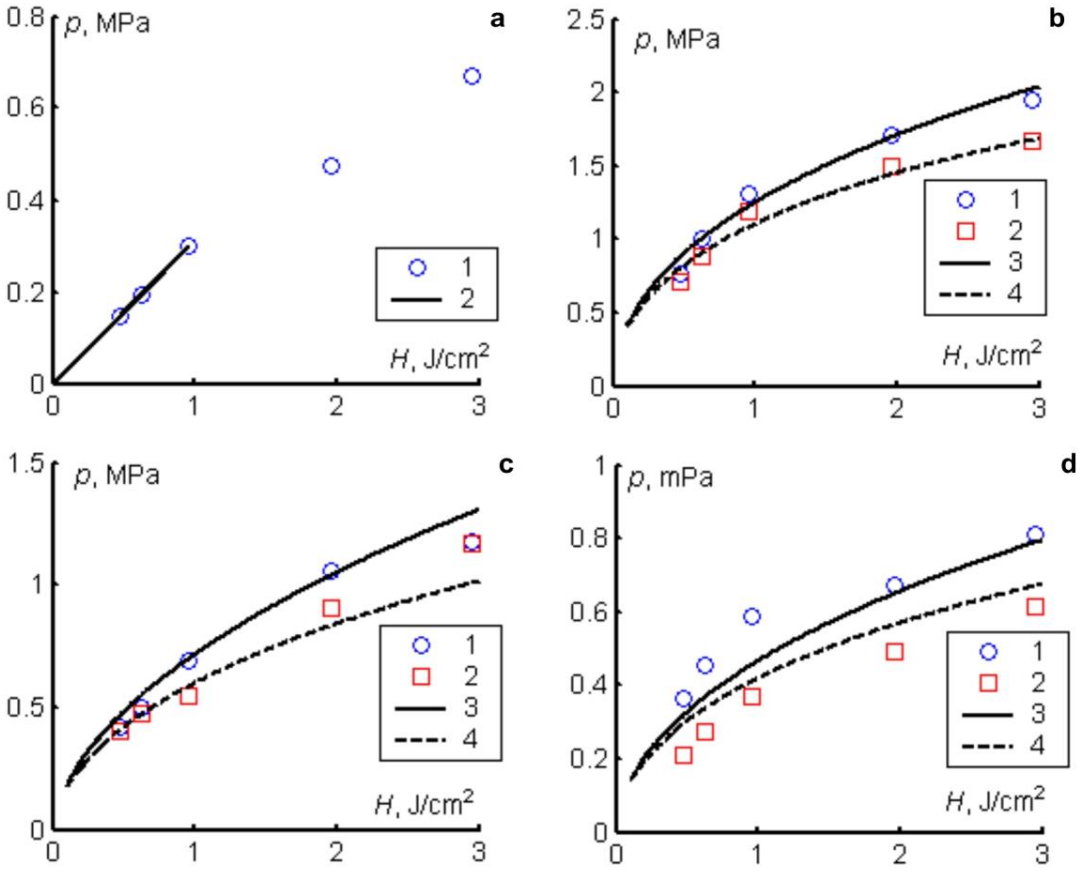

Figure 5. The photoacoustic signal amplitude dependence on the pulse energy density in the cases of ferrocene (a) and colloid ablation products of aluminum (b), nickel (c), and zinc (d) targets. On the "a" part 1 is experiment and 2 is linear approximation, while on others 1 and 2 are experimental data and 3 and 4 are approximation using model (5).

The dependence is linear up to 1 J/cm^2 in the ferrocene case. The sublinear character at higher energy densities arises due to optical breakdown on the bubbles and uncontrolled impurities. The photoacoustic signal amplitude dependence on the energy density is substantially sublinear in the cases of colloid obtained

with metal targets' ablation in the entire studied range. The linear type of the dependence at low energy densities allowed us to estimate the calibration coefficient linking pressure and signal amplitudes at 101 kPa/mV.

We approximated the photoacoustic signal amplitude in the studied colloids case as:

$$p = \int_{x_0}^{x_0+a} \eta(x)\frac{dH(x)}{dx}dx = \int_{H(x_0)}^{H(x_0+a)} \eta(H)dH. \quad (4)$$

Equation (4) assumes that the transformation of the laser energy into the pressure wave has the efficiency η. The transformation is sensible in the range with *a* width only. In the linear range η = const. We assumed, that the efficiency is a power function of the energy density in the attenuation becomes non-linear ($H > H_c$) $\eta = \eta_b \cdot (H/H_b)^{-m}$, where H_b is "basic" energy density value taken as 0.2 J/cm^2, so $\eta = \eta_b$, if $H = H_c$.

The linear absorption range is not reached in the case of photoacoustic measurements; the energy density falling inside the cuvette is described with the lowest part of the formula (2). Having taken the integral in (4) one gets:

$$p = \frac{\eta_b H_b}{1-m} \cdot \left[\left(\frac{H(x_0)}{H_b} \right)^{1-m} - \left(\frac{H(x_0+a)}{H_b} \right)^{1-m} \right]. \quad (5)$$

The approximation results of the experimental dependencies of photoacoustic response amplitude on energy density of the laser pulse are shown in Figure 5; the approximation parameters are presented in Table 2.

Table 2

Approximation parameters for μ(*H*) and η(*H*) dependencies

sample source	μ, cm^{-1} (spectrophotometry)	z-scan			photoacoustics			
		μ, cm^{-1}	*n*	H_c, mJ/cm^2	*n*	H_c, mJ/cm^2	η_b, cm^{-1}	*m*
Al	1.37	1.34	1.79	288	0.47	22.9	9.71	0.94
Ni	0.692	0.379	1.41	336	0.39	1.21	4.06	0.75
Zn	0.811	0.849	0.902	241	0.47	14.3	4.39	0.91

Discussion

The experimental dependencies of the transmittance on the pulse energy density in the case of colloid ablation products evidence the substantially non-linear light attenuation. The simple model based on the energetic threshold describes the results well (Fig. 3). An interesting feature is this threshold decreasing as a dilution result. The power value in the respective law is not a positive integer number, which decreases with dilution. The dependence of the equation (1) parameters on the colloid concentration observed cannot arise if the laser light absorption centers act independently. The threshold of non-linear attenuation H_c decreasing after dilution is reasonable if the interaction becomes weaker with the distance between centers increasing.

One discerns the influences of the optic properties and absorbed energy transformation. The efficiency parameter could be written as $\eta(H) = \mu_a\gamma$. In the case of solids thermal expansion the dimensionless parameter γ is known as Grüneisen parameter that can be estimated as $\rho c_s^2\beta/c_p$. The respective value for DMSO is 0.99 [19] which is close to typical value about 1 for most of the substances. In the low energy density range the value of η is higher than 1. For instance, at H =150 mJ/cm^2 the efficiency value is 12.7, 5.04, and 5.70 cm^{-1} for colloid obtained with aluminum, zinc, and nickel targets' ablation respectively. Estimating the linear absorption coefficient roughly as the attenuation one, we may estimate the respective values for γ as 39, 22, and 23 respectively for the same samples. The attenuation is the sum of absorption and scattering processes, so real γ should be even higher. So high values could be reached, if the substance undergoes phase transitions accompanied by significant expansion, such as evaporation and sublimation. These considerations agree with the parameters H_c and *n* of the equation (1) decreasing after dilution. The decreasing in concentration means increasing of the average solvent volume containing one light absorbing center. The typical acoustic relaxation time of the excited area is $w/c_s \approx 160$ ns, which is an order of magnitude higher than the

pulse duration. On the other hand, estimating the typical concentration of nanoparticles using average diameter, one founds the acoustic relaxation time between nanoparticles about 1 ns. Thus, the irradiation zone cannot increase its volume significantly during the pulse, so pressure increasing due to gases formation has to be linked with the respective solvent contraction. In the pressure range experimentally estimated the 12.5 times dilution has led to pressure drop in the system 12.5 times at the same gas phase volume. The pressure increasing shifts the evaporation and sublimation equilibrium toward the condensed phase formation. This way, the decreasing in H_c after dilution agrees with the phase transitions influence on the qualitative level. Formation of the gas phase around the light absorbing centers leads to the increasing in their scattering cross section that agrees with transmittance decreasing when the energy density of the laser pulse increases (Fig. 3).

The influence of the nanoparticles' concentration is seldom discussed as the parameter influencing the non-linear light attenuation. The effects discussed have some similarities with laser initiation of the secondary explosives doped with metal nanoparticles. It was shown in [20] that the minimal energy density is achieved for the nanoparticles' concentration providing the maximum of pressure measured with photoacoustic techniques in the under threshold mode. The gas phase formation is highly endothermic becoming a fast means of the energy dissipation. If the pressure increases when the nanoparticles are heated with the laser pulse, this increasing inhibits the sublimation and evaporation, making the temperature in the reaction hot-spots increase and threshold energy density of explosion decrease [20].

In the case of zinc target ablation products and photoacoustic sensor position near the front of the cuvette the pressure values vary in the vide range. The pressure amplitude on the energy density dependence for both sensor positions is poorer than in the aluminum and nickel cases. We suggest that in the zinc case the optic breakdown begins at the front of the cuvette. The zinc sulfide colloids are able to self-focus the laser beams [21] that increase the effective energy density. The breakdown is a probabilistic event that can explain high dispersion of the pressure amplitudes. Stronger laser light attenuation in the breakdown area making the pressure increase in the front area decreases it in the middle one hindering the description of both curves with one set of parameters.

Conclusion

Metal targets ablation in the liquid medium allows one to obtain colloid with strong non-linear light attenuation. In the present paper we proved that photoacoustic data are important for the nature of the non-linear absorption detection. The photoacoustic results and influence of the concentration on the non-linear absorption parameters exclude such mechanisms of non-linear absorption as two-photon and two-step absorption. At the same time, the formation of the gas phase due to heating and subsequent evaporation and sublimation of the matter qualitatively agrees with the effects observed.

References

1 Ganeev, R.A. (2019). Characterization of the Optical Nonlinearities of Silver and Gold Nanoparticles. *Optics and Spectroscopy*, 127, 487–507. https://doi.org/10.1134/S0030400X19090108

2 Majles Ara, M.H., Dehghani, Z., Sahraei, R., Daneshfar, A., Javadi, & Z., Divsar, F. (2012). Diffraction patterns and nonlinear optical properties of gold nanoparticles. *Journal of Quantitative Spectroscopy & Radiative Transfer*, 113, 366–372. https://doi.org/10.1016/j.jqsrt.2011.12.006

3 Fathima, R., Mujeeb, A. (2021). Plasmon enhanced linear and nonlinear optical properties of natural curcumin dye with silver nanoparticles. *Dyes and Pigments*, 189, 109256. https://doi.org/10.1016/j.dyepig.2021.109256

4 Ovchinnikov, O.V., Smirnov, M.S., Chevychelova, T.A., Zvyagin, A.I., & Selyukov, A.S. (2022). Nonlinear absorption enhancement of Methylene Blue in the presence of Au/SiO2 core/shell nanoparticles. *Dyes and Pigments*, 197, 109829. https://doi.org/10.1016/j.dyepig.2021.109829

5 Fathima, R., & Mujeeb, A. (2021). Enhanced nonlinear and thermo optical properties of laser synthesized surfactant-free Au-Pt bimetallic nanoparticles. *Journal of Molecular Liquids*, 343, 117711. https://doi.org/10.1016/j.molliq.2021.117711

6 Silva-Silva, T.P., Silva, A.A., Oliveira, M.Ch.D., Souza, P.R., Silva-Filho, E.C., Garcia, H.A., Costa, J.C.S., & Santos, F.E.P. (2023). Biosynthesis of Ag@Au bimetallic nanoparticles from Hymenaea courbaril extract (Jatoba) and nonlinear optics properties. *Journal of Molecular Liquids*, 389, 122641. https://doi.org/10.1016/j.molliq.2023.122641

7 Al–Ghamdi, H., Aloraini, D.A., Almuqrin, A.H., Jagannath, G., & Sayyed, M.I. (2024). Nanosecond nonlinear optical properties of oxide glasses embedded with plasmonic nanoparticles at the spectral excitation near to surface plasmon resonance. *Physica B*, 678, 415756. https://doi.org/10.1016/j.physb.2024.415756

8 Guzman-Barraza, A., Ortega-Mendoza, J.G., Padilla-Vivanco, A., Arroyo Carrasco, M.L., Silva-Gonzalez, N.R., Zaca-Moran, P., & García Ramírez, E.V. (2024). Characterization of the nonlinear optical properties of Zn and Ag nanoparticles using light at 1550 nm. *Results in Optics*, 14, 100590. https://doi.org/10.1016/j.rio.2023.100590

9 Gusev, V.E., & Karabutov, A.A. (1992). *Laser Optoacoustics*. N.Y. American Institute of Physics, 296 p.

10 Bialkowski, S.E., Astrath, N.G.C., & Proskurnin, M.A. (2019). *Photothermal Spectroscopy Methods*. John Wiley & Sons, 512 p.

11 Amendola, V., Polizzi, S., & Meneghetti, M. (2006). Laser Ablation Synthesis of Gold Nanoparticles in Organic Solvents. *Journal of Physical Chemistry B*, 110, 7232–7237. https://doi.org/10.1021/jp0605092

12 Bozon-Verduraz, F, Brayner, R., Voronov, V.V., Kirichenko, N.A., Simakin, A.V., & Shafeev, G.A. (2003). Production of nanoparticles by laser-induced ablation of metals in liquids. *Quantum Electronics*, 33, 714–720. https://doi.org/10.1070/QE2003v033n08ABEH002484

13 Podagatlapalli, G.K., Hamad, S., Sreedhar, S., Tewari, S.P., & Rao, S.V. (2012). Fabrication and characterization of aluminum nanostructures and nanoparticles obtained using femtosecond ablation technique. *Chemical Physics Letters*, 530, 93–97. https://doi.org/10.1016/j.cplett.2012.01.081

14 Shiju, E., Siji, N.N.K, Narayana, R.D., & Chandrasekharan, K. (2020). Enhanced nonlinear absorption and efficient power limiting action of Au/Ag@ graphite core-shell nanostructure synthesized by laser ablation. *Nano Express*, 1, 030026. https://doi.org/10.1088/2632-959X/abca0f

15 Aleali, H., Sarkhosh, L., Karimzadeh, R., & Mansour, N. (2011). Optical limiting response of Ag2S nanoparticles synthesized by laser ablation of silver target in DMSO. *Phys. Status Solidi B*, 248(3), 680–685. https://doi.org/10.1002/pssb.201046107http://database.iem.ac.ru/mincryst/rus/index.php

16 Wang, G., Huang, B., Li, Zh., Lou, Z., Wang, Z., Dai, Y., & Whangbo, M.H. (2015). Synthesis and characterization of ZnS with controlled amount of S vacancies for photocatalytic H2 production under visible light. *Scientific Reports*, 5, 8544. https://doi.org/10.1038/srep08544

17 Dehghani, Z., Nazerdeylami, S., Saievar-Iranizad, E., & Majles Ara, M.H. (2011). Synthesis and investigation of nonlinear optical properties of semiconductor ZnS nanoparticles. *Journal of Physics and Chemistry of Solids*, 72, 1008–1010. https://doi.org/10.1016/j.jpcs.2011.05.005

18 Watcher (Ed.) (1998). *Kirk-Othmer Encyclopedia of Chemical Technology* (Vol. 23, 4th edition). John Wiley & Sons. 107-108.

19 Aduev, B.P., Nurmukhametov, D.R., Zvekov, A.A., Nikitin, A.P., & Kalenskii, A.V. (2016). Laser initiation of petn-based composites with additives of ultrafine aluminium particles. *Combustion, Explosion, and Shock Waves, 52*(6), 713–718. https://doi.org/10.1134/S0010508216060113

20 Ganesha Krishna, V.S., & Mahesha, M.G. (2022). "ZnS, an excellent material in photonics" — A review based on Z-scan study. *Physica B*, 628, 413628. https://doi.org/10.1016/j.physb.2021.413628

А.А. Звеков, А.В. Каленский, А.В. Иванов, А.П. Боровикова, Д.Р. Нурмухаметов

Диметилсульфоксидтегі металл нысандарының лазерлік абляциясымен дайындалған коллоидтардың сызықтық емес оптикалық қасиеттері

Алюминий, никель және мырыш негізіндегі коллоидты ерітінділер диметилсульфоксид ортасында тиісті металл нысандарын абляциялау арқылы алынды. Үлгілер ультракүлгін УК-*вис* спектроскопиясы, трансмиссиялық электронды микроскопия және динамикалық жарық шашырау әдістерімен зерттелді. Импульсті неодим лазерін (532 нм, 14 нс) қолдана отырып, z-сканерлеу әдістерімен айтарлықтай сызықтық емес әлсіреу байқалды. Жарық қарқындылығы жоғарылаған сайын үлгілердің өткізгіштігі төмендейді. Оптоакустикалық сигналдың амплитудасы сәулелену қарқындылығының жоғарылауымен сызықтық түрде өсті. Ферроцен ерітіндісін стандарт ретінде қолдану абсолютті бірліктердегі қысым амплитудасының шамаларын алуға мүмкіндік берді. Оптоакустикалық сигналдың өткізгіштігі мен амплитудасының импульстік энергия тығыздығына тәуелділігін сипаттау үшін әсер ету шегі бар қуат заңдары қолданылды. Коллоидты ерітінділерді сұйылту кезінде өзгеретін тәуелділік параметрлері бағаланды. Шың қысымының шамалары қыздырылған кезде үлгінің сызықтық кеңеюін қарастыратын классикалық оптоакустикалық эффект теориясының бөлігі ретінде түсіндіруге болмайтындығы көрсетілген. Нәтижелерді талқылау үшін заттың буланыуна және оларды қыздыру кезінде нанобөлшектердің айналасында бу көпіршіктерінің пайда болуына негізделген сызықтық емес әлсіреу механизмі тартылады, ол сапалы деңгейде оптоакустикалық сигнал амплитудасының энергия тығыздығына субсызықтық тәуелділігіне сәйкес келеді.

Кілт сөздер: абляция, диметилсульфоксид, жарықтың сызықты емес әлсіреуі, фотоакустикалық спектроскопия, лазерлік сәулелену.

А.А. Звеков, А.В. Каленский, А.В. Иванов, А.П. Боровикова, Д.Р. Нурмухаметов

Нелинейные оптические свойства коллоидных продуктов абляции металлических мишеней в диметилсульфоксиде

Коллоидные растворы на основе алюминия, никеля и цинка были получены абляцией соответствующих металлических мишеней в среде диметилсульфоксида. Образцы были исследованы методами УФ-*вис* спектроскопии, просвечивающей электронной микроскопии и динамического рассеяния света. Существенное нелинейное ослабление излучения неодимового лазера (532 нм, 14 нс) было обнаружено методом *z*-сканирования, причем наблюдалось падение пропускания при приближении к фокусу. Амплитуда оптоакустического сигнала увеличивалась сублинейно при росте интенсивности излучения. Применение раствора ферроцена в качестве стандарта позволило получить величины амплитуды давления в абсолютных единицах. Для описания зависимостей коэффициента пропускания и амплитуды оптоакустического сигнала от плотности энергии импульса использовались степенные законы с порогом появления эффекта. Были оценены параметры зависимостей, которые изменяются при разбавлении коллоидных растворов. Показано, что величины пикового давления не могут быть интерпретированы в рамках классической теории оптоакустического эффекта, рассматривающей линейное расширение образца при нагревании. Для обсуждения результатов привлекается механизм нелинейного ослабления, основанный на испарении вещества и формировании пузырьков паров вокруг наночастиц при их нагреве, который на качественном уровне согласуется с сублинейной зависимостью амплитуды оптоакустического сигнала от плотности энергии.

Ключевые слова: абляция, диметилсульфоксид, нелинейное ослабление, фотоакустическая спектроскопия, лазерное излучение.

Information about the authors

Alexander Zvekov (corresponding author) — Doctor of physical and math science, Professor, Department of Solid State Chemistry and Material Science, Kemerovo State University, Krasnaya st., 6, 650000, Kemerovo, Russia; *e-mail*: *zvekovaa@gmail.com*, https://orcid.org/0000-0002-2941-9783

Alexander Kalenskii — Doctor of physical and math science, Head of the Department of Solid State Chemistry and Material Science, Kemerovo State University, Krasnaya st., 6, 650000, Kemerovo, Russia; *e-mail: kalenskyav@gmail.com*; https://orcid.org/0000-0002-6658-0787

Alexey Ivanov — 3rd year PhD student, Kemerovo State University, Krasnaya st., 6, 650000, Kemerovo, Russia; e-mail: *alecs-2004@yandex.ru*

Anastasia Borovikova — Candidate of physical and math science, Head of the Scientific and Innovation Office, Kemerovo State University, Krasnaya st., 6, 650000, Kemerovo, Russia; e-mail: *science@kemsu.ru*, https://orcid.org/0000-0002-4987-3406

Denis Nurmuhametov — Doctor of physical and math science, Head of the Institute of coal Chemistry and Material Science, Federal Research Center of Coal and Coal Chemistry SB RAS, Sovetsky av., 18, 650000, Kemerovo, Russia; e-mail: *ndr999@gmail.com*